Identification of Optimal Capacity of MACST Facilities for Risk Reduction under Combined Earthquake-Tsunami Hazard

Minkyu Kim [a], Eujeong Choi [a*], Seunghyun Jang [a], Daegi Hahm [a]
[a] *Structural and Seismic Safety Research Division, Korea Atomic Energy Research Institute, 111, Daedeok-daero 989beon-gil, Yuseong-gu, Daejeon, Republic of Korea 34057*
[*] *Corresponding author: ejchoi@kaeri.re.kr*

***Keywords :** Nuclear power plants, MACST, Optimal capacity, Combined earthquake-tsunami hazard, I-DQFM.

1. Introduction

The Fukushima nuclear disaster in 2011 revealed the vulnerability of nuclear power plants (NPPs) to combined natural disasters, particularly earthquakes and tsunamis. This catastrophic event highlighted the severe challenges that nuclear facilities face in dealing with combined hazards that exceed their original design basis. The simultaneous occurrence of multiple severe natural hazard events, as seen in the Fukushima disaster where cooling systems failed due to the tsunami following the earthquake, can overburden safety systems, leading to severe consequences such as core damage and radioactive release.

Despite advances in nuclear safety protocols, there are still significant gaps in the ability of nuclear power plants to effectively manage combined hazards. Traditional safety measures often address single hazard scenarios, such as an earthquake or a tsunami alone, without adequately considering the combined effects of simultaneous events. This can lead to underestimated risks and inadequate preparedness. In addition, climate change is increasing the frequency and intensity of natural disasters, making the development of comprehensive safety strategies even more critical.

To address these challenges, Korea Hydro & Nuclear Power Co., Ltd (KHNP) has implemented the Multi-barrier Accident Coping Strategy (MACST) in response to the implementation of the Diverse and Flexible Coping Strategies (FLEX) in the US [1]. MACST is designed to cope with all possible accidents at NPPs, from design basis to beyond-design-basis events, including extreme natural hazards. The strategy includes new equipment, dedicated organizations, improved procedures, and comprehensive training programs. Key safety goals of MACST include reducing the frequency of severe accidents (Core Damage Frequency, CDF) to less than once in 10,000 years, reducing the frequency of containment failures (Large Early Release Frequency, LERF) to less than once in 100,000 years, and limiting the release of significant radioactive isotopes to less than once in one million years.

However, despite the implementation of MACST, several issues remain to be addressed. First, there is a lack of quantitative assessment of the risk reduction effects of MACST facilities in extreme events after implementation. In addition, there are no established optimal capacity standards for MACST facilities under various disaster conditions. This limits the ability to ensure consistent and reliable performance of these facilities during extreme events.

Therefore, the objective of this study is to evaluate the risk reduction provided by MACST facilities in both single earthquake and combined earthquake-tsunami hazards, with a focus on the OPR1000 and APR1400 NPP systems. Specifically, the study targets two MACST facilities, the 1.0 MW large capacity mobile generator and the mobile low-pressure pump. Using the Improved Direct Quantification of Fault Tree with Monte Carlo Simulation (I-DQFM) method for risk assessment, this study provides a detailed analysis of the vulnerability and performance of NPPs under combined hazard conditions with MACST facilities. The study also proposes optimal capacities for MACST facilities, focusing on their capacities for seismic and tsunami resistance, thereby contributing to ongoing efforts to improve nuclear safety and resilience in an increasingly unpredictable environment.

2. Risk Assessment Methods and Hazard Scenarios

This section describes the risk assessment methodology and details the hazard scenarios considered in this study. The I-DQFM method is used to extend the traditional Probabilistic Safety Assessment (PSA) to efficiently quantify multi-hazard risks. The construction method of the correlation matrices, which is used in the I-DQFM method, for the components of the OPR1000 and APR1400 NPP systems is outlined. In addition, the single earthquake hazard and the combined earthquake-tsunami hazard scenarios are detailed to demonstrate the application of these methods in the evaluation of the core damage risk.

2.1 Combined hazard risk assessment using I-DQFM

For the safety analysis of nuclear facilities, most of the risk quantification methods developed previously have been developed for single external-hazard events. Therefore, an extension of the existing single-hazard External Event PSA (EE-PSA) methodology is essential for quantifying the risk of nuclear facilities for multiple hazards. Conceptually, multi-hazard risk quantification can be expressed in the following equation:

$$Risk = \int_0^\infty \cdots \int_0^\infty F(a_1, \cdots, a_n) \left| \frac{dH(a_1, \cdots, a_n)}{da_1 \cdots da_n} \right| da_1 \cdots da_n \quad (1)$$

where a_i represents the hazard intensity of each considered external hazard i. In the case of a single external hazard event, the external event hazard information *H* and the system fragility information *F* are expressed as a one-dimensional function in a conventional single external hazard event, and the corresponding final risk is quantified by the one-dimensional integral. In multi-hazard risk quantification, however, the hazard and fragility are expressed in a multi-dimensional space, and the final risk is quantified by multi-dimensional integration.

The DQFM method is a traditional approach used in PSA the risk quantification associated with NPPs [2]. It involves the use of fault tree analysis to evaluate the probability of different failure scenarios. The DQFM method calculates failure probabilities by considering individual component failures and their contributions to system-level failures. This approach typically uses Boolean algebra to model the logical relationships between component failures and system failures. While effective for single-hazard scenarios, DQFM is limited in its ability to handle multi-hazard scenarios due to its inability to account for partial dependencies and the combined effects of different hazards on the system.

To address these limitations, the I-DQFM was developed [3]. I-DQFM extends traditional PSA to efficiently quantify multi-hazard risks by combining probability distribution-based Boolean algebraic approaches with sampling-based methods. This improvement significantly improves computational efficiency and accuracy by more effectively handling partial dependencies between system components.

The process begins with the input of fault tree data and component fragility data for external hazards, such as earthquakes and tsunamis. The fragility parameters such as median hazard capacities $(\mathbf{A}_{ms}, \mathbf{A}_{mt})$, log-normal standard deviations which indicate randomness and uncertainty $(\boldsymbol{\beta}_{rs}, \boldsymbol{\beta}_{rt}, \boldsymbol{\beta}_{us}, \boldsymbol{\beta}_{ut})$, and correlation coefficients $(\boldsymbol{\rho}_s, \boldsymbol{\rho}_t)$ are defined. The composite log-normal standard deviations of each hazard $\boldsymbol{\beta}_{cs}$ and $\boldsymbol{\beta}_{ct}$ can be calculated as:

$$\boldsymbol{\beta}_{cs} = \sqrt{\boldsymbol{\beta}_{rs}^2 + \boldsymbol{\beta}_{us}^2} \quad (2)$$

$$\boldsymbol{\beta}_{ct} = \sqrt{\boldsymbol{\beta}_{rt}^2 + \boldsymbol{\beta}_{ut}^2} \quad (3)$$

Then, as suggested by Reed et al. (1985), these composite standard deviations can be decomposed into log-standard deviations for response and capacity as follows [4]:

$$\boldsymbol{\beta}_{Rcs} = \boldsymbol{\beta}_{Ccs} = \sqrt{\frac{\boldsymbol{\beta}_{cs}^2}{2}} \quad (4)$$

$$\boldsymbol{\beta}_{Rct} = \boldsymbol{\beta}_{Cct} = \sqrt{\frac{\boldsymbol{\beta}_{ct}^2}{2}} \quad (5)$$

Next, N samples are generated for the response $(\mathbf{R}_{Ms}, \mathbf{R}_{Mt})$ and capacity $(\mathbf{C}_s, \mathbf{C}_t)$ distributions for each hazard as follows:

$$\mathbf{R}_{Ms} \sim LN(\mathbf{A}_{ms}, \boldsymbol{\beta}_{Rcs}, \boldsymbol{\rho}_s) \quad (6)$$

$$\mathbf{R}_{Mt} \sim LN(\mathbf{A}_{mt}, \boldsymbol{\beta}_{Rct}, \boldsymbol{\rho}_t) \quad (7)$$

$$\mathbf{C}_s \sim LN(\mathbf{A}_{ms}, \boldsymbol{\beta}_{Ccs}, \boldsymbol{\rho}_s) \quad (8)$$

$$\mathbf{C}_t \sim LN(\mathbf{A}_{mt}, \boldsymbol{\beta}_{Cct}, \boldsymbol{\rho}_t) \quad (9)$$

Hazard intensity levels **a** and **h** are then defined for each hazard. The process iterates for each hazard intensity level i, scaling the responses accordingly:

$$\mathbf{R}_s = \mathbf{R}_{Ms}\left(\frac{\mathbf{a}_i}{\mathbf{A}_{ms}}\right) \quad (10)$$

$$\mathbf{R}_t = \mathbf{R}_{Mt}\left(\frac{\mathbf{h}_i}{\mathbf{A}_{mt}}\right) \quad (11)$$

Components are judged for failure by comparing the scaled responses to the capacities ($R_i > C_i$, $R_j > C_j$, and $R_i > C_i$ or $R_j > C_j$). Using the binary states of components (safe or fail), failures of subsystems (intermediate events) and the entire system (top event) are judged using fault tree analysis. Failure probabilities for components, subsystems, and the entire system are evaluated given hazard intensities (F/N, where F is the total number of failures and N is the total number of samples). A multi-hazard system fragility curve is then developed for components, subsystems, and the overall system. Finally, risk quantification and other post-processing steps are performed to derive the annual CDF and other relevant risk metrics. By following these steps, the I-DQFM method provides a comprehensive and efficient framework for multi-hazard risk assessment.

2.2 NPP Systems with MACST Facilities

The methodology is applied to the OPR1000 and APR1400 NPP systems, addressing the general multi-hazard problems of actual NPPs. In the NPP system models, the MACST facilities, the 1.0 MW large capacity mobile generator and the mobile low-pressure pump, are added to evaluate the risk reduction effectiveness of each facility under both single and combined hazard scenarios.

For the OPR1000 and APR1400 NPPs, the fragility parameters are defined, including median hazard capacities, $\mathbf{A}_{ms}$ and $\mathbf{A}_{mt}$, log-normal standard deviations, $\boldsymbol{\beta}_{rs}, \boldsymbol{\beta}_{rt}, \boldsymbol{\beta}_{us}$ and $\boldsymbol{\beta}_{ut}$, and correlation

matrices. Tables 1 and 2 provide detailed information on the multi-hazard component fragility and random failure probability for the OPR1000 and APR1400 NPPs, respectively. Here, due to unavailability of information, it is assumed that $\boldsymbol{\beta}_{rt}$ and $\boldsymbol{\beta}_{ut}$ are equal, thus only the composite standard deviation $\boldsymbol{\beta}_{ct}$ is presented. Also, "NO" denotes $\mathbf{A}_{mt}$ of the components not affected by the tsunami, and the capacities of the MACST facilities are denoted as "*param.*" since they are varied to assess the risk reduction effectiveness.

In addition, event trees are constructed for both NPPs to evaluate the sequence of events following an initiating hazard event. In the OPR1000 model shown in Fig. 1, six core damage accident scenarios are considered. Among these scenarios, Loss of Essential Power (LEP) is an accident in which power supply equipment for accident mitigation, such as 4.16kV switchgear and 480V load center, is damaged. Thus, the power supply by 1MW mobile generator is considered in this scenario, and it is assumed that core damage would occur if this operation fails. And since the Loss of Secondary Heat Removal (LHR) is an accident in which feed-water to the steam generator is lost due to damage to the condensate storage tank, the injection of feed-water into the steam generator by a mobile low-pressure pump is considered. For Loss of Off-site Power (LOOP) and General Transients (GTRN), additional accident mitigations are considered and failure probabilities of 1.24×10^{-2} and 1.25×10^{-3}, respectively, are assumed. The other scenarios, Loss of Component Cooling Water (LOCCW) and Small Loss of Coolant Accident (SLOCA), assume direct core damage without additional accident mitigation.

For the APR1400 model, seven accident scenarios of core damage are considered, as shown in Fig. 2. In case of LEP accident, the power supply by 1MW mobile generator is considered in the same way as in the OPR1000 model. Additional accident mitigations for LOCCW and Loss of Component Control System (LOC) are considered, and the failure probability of these mitigations is assumed to be 6.83×10^{-3}. After failure of the accident mitigation measures, the injection of feed-water into the steam generator by a mobile low-pressure pump is considered. In addition, failure probabilities of additional accident mitigation measures are assumed to be 1.25×10^{-3} for SLOCA and GTRN and 1.24×10^{-2} for LOOP. For the Large Loss of Coolant Accident (LLOCA), it is assumed that the core damage would occur directly without additional accident mitigation.

Table 1. Multi-hazard component fragility and random failure probability information of the OPR1000 NPP.

Components	**Seismic Event**			**Tsunami Event**	
	$\mathbf{A}_{ms}$	$\boldsymbol{\beta}_{rs}$	$\boldsymbol{\beta}_{us}$	$\mathbf{A}_{mt}$	$\boldsymbol{\beta}_{ct}$
Auxiliary Building	2.00	0.32	0.37	10	0.3
Switches	2.33	0.41	0.45	11	0.3
HVAC Ducting and Supports	2.06	0.32	0.41	NO	-
Emergency diesel generator	1.13	0.36	0.30	11	0.3
4.16kV Switchgear (functional)	1.33	0.33	0.30	11	0.3
480V load center (functional)	1.50	0.32	0.29	11	0.3
Battery charger (functional)	1.03	0.28	0.28	11	0.3
Inverter (functional)	1.37	0.33	0.30	11	0.3
Regulating transformer (functional)	1.30	0.33	0.30	11	0.3
125V DC control center	1.58	0.33	0.29	11	0.3
Battery charger (structural)	1.54	0.33	0.33	11	0.3
Battery rack (structural)	1.46	0.33	0.31	NO	-
Essential Chilled Water (ECW) compression tank	1.00	0.35	0.20	11	0.3
ECW chiller	1.08	0.28	0.27	11	0.3
ECW pump	1.85	0.36	0.27	11	0.3
Component cooling water surge tank	2.00	0.41	0.47	NO	-
480V motor control center (functional)	1.33	0.33	0.30	NO	-
480V motor control center (structural)	1.99	0.33	0.33	NO	-
Essential service water pump	1.20	0.29	0.28	11	0.3
Condensate storage tank	1.044	0.25	0.242	10	0.3

Off-site power	0.30	0.22	0.20	10	0.3
Instrumentation Tube	1.50	0.30	0.30	NO	-
1.0 MW large capacity mobile generator	*param.*	0.30	0.30	*param.*	0.3
Mobile low-pressure pump	*param.*	0.30	0.30	*param.*	0.3

Table 2. Multi-hazard component fragility and random failure probability information of the APR1000 NPP.

Components	**Seismic Event**			**Tsunami Event**	
	$\mathbf{A}_{ms}$	$\boldsymbol{\beta}_{rs}$	$\boldsymbol{\beta}_{us}$	$\mathbf{A}_{mt}$	$\boldsymbol{\beta}_{ct}$
Emergency diesel generator	1.00	0.34	0.19	11	0.3
4.16kV switchgear (functional)	1.13	0.32	0.40	11	0.3
Regulating transformer (structural)	1.40	0.32	0.44	11	0.3
125V DC control center	1.45	0.32	0.43	11	0.3
Inverter (structural)	1.45	0.34	0.33	11	0.3
480V motor control center (structural)	0.89	0.34	0.33	11	0.3
Component control system cabinet	1.09	0.36	0.35	NO	-
Instrumentation tube	1.50	0.30	0.30	NO	-
Off-site power	0.20	0.20	0.25	10	0.3
Component cooling water heat exchanger	1.02	0.35	0.25	11	0.3
1.0 MW large capacity mobile generator	*param.*	0.30	0.30	*param.*	0.3
Mobile low-pressure pump	*param.*	0.30	0.30	*param.*	0.3

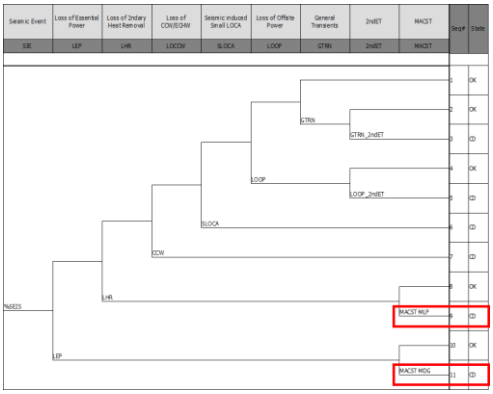

Fig. 1. Event tree for OPR1000 with MACST facilities.

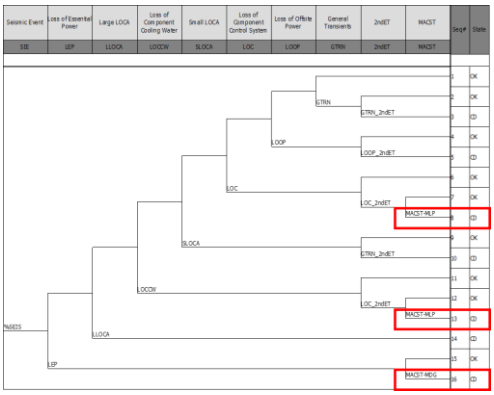

Fig. 2. Event tree for APR1400 with MACST facilities.

2.3 Correlation Matrices of System Components for Seismic and Tsunami Hazards

To accurately assess the risk of multi-hazard scenarios, it is important to consider the correlation between different system components. The correlation matrix represents the dependency between the responses of different components under seismic and tsunami hazards.

Eem et al. (2021) proposed a method to construct a correlation matrix specifically for Korean NPPs under seismic hazard [5]. The matrix depends on both the floor location and the natural frequency of the components, with correlation coefficients set based on these factors. For components on the same floor, the correlation coefficient is set to 1.0 for the same natural frequency and 0.89 for different natural frequencies. For components on different floors, the correlation coefficient is 0.74 for same natural frequency and 0.68 for different natural frequencies. The correlation matrices of OPR1000 and APR1400 for seismic hazard are shown in Fig. 3 and Fig. 4, respectively.

For tsunami hazard, the correlation coefficients for components installed in the same building or site are 1.0, indicating perfect correlation. For components installed in different locations, the correlation coefficient is 0, indicating no correlation. These correlation values are

essential for accurately modeling the joint probability of failure of multiple components, leading to a more realistic assessment of the overall system vulnerability. The correlation matrices for tsunami hazard are shown in Fig. 5 and Fig. 6, respectively.

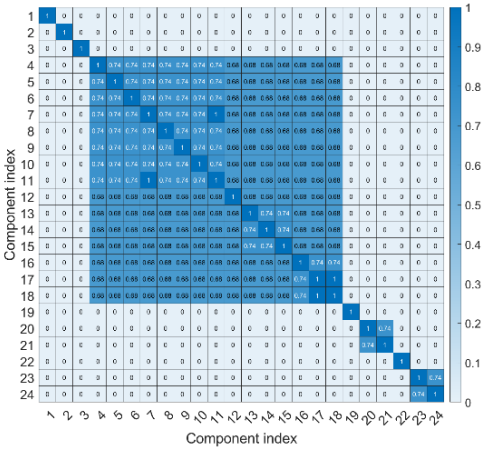

Fig. 3. Correlation matrix of OPR1000 for seismic hazard.

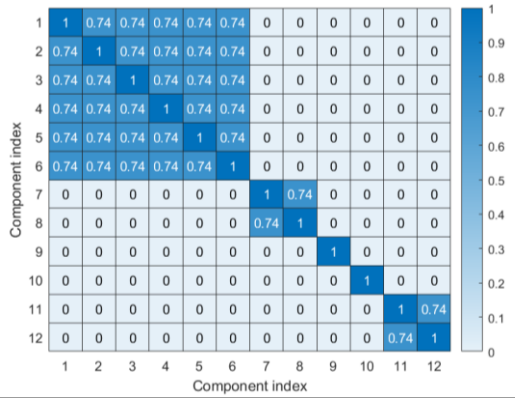

Fig. 4. Correlation matrix of APR1400 for seismic hazard.

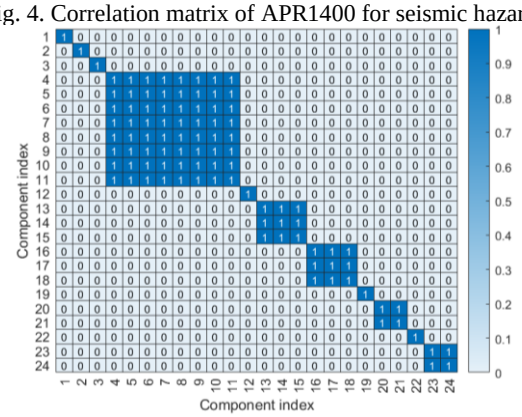

Fig. 5. Correlation matrix of OPR1000 for tsunami hazard.

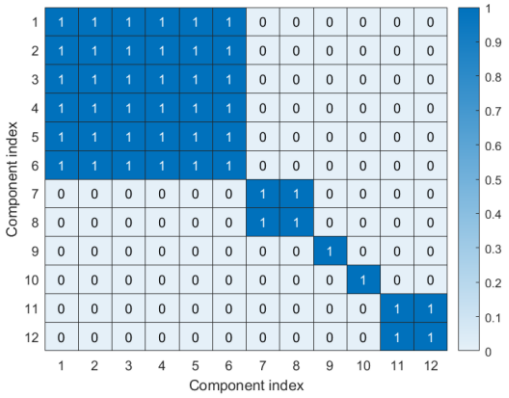

Fig. 6. Correlation matrix of APR1400 for tsunami hazard.

2.4 Hazard Scenarios and Capacity Evaluation of MACST Facility

The core damage risk for OPR1000 and APR1400 NPP systems is evaluated using I-DQFM method under both single hazard (earthquake) and combined hazard (earthquake and tsunami) scenarios. The methodology involves a parametric study in which the capacities of the MACST facilities, the 1.0 MW large capacity mobile generator and the mobile low-pressure pump, are varied to assess their effectiveness in reducing risk and to identify optimal capacity standards for each scenario. Risk assessments are performed at all points within the specified ranges to evaluate the effectiveness of risk reduction at each capacity level. The objective is to determine the optimal capacities that minimize the risk of core damage, assuming that the capacity of each facility is identical.

For the single hazard scenario, the seismic hazard maps used in Ellingwood (1990), as shown in Fig. 7, are introduced [6]. In this study, earthquake hazard maps of six seismogenic zones with intensities ranging from 0.05 g to 2.0 g with an interval of 0.01 g are used. The risk assessments incorporate these hazard maps by applying weights based on the annual exceedance probability of the effective peak ground acceleration (PGA). The capacities of the MACST facilities, the 1.0 MW large capacity mobile generator and the mobile low-pressure pump, are varied in the range of 0.01 g to 3.0 g with 0.01 g intervals to evaluate the risk reduction effectiveness and to determine the optimal seismic capacity.

In the combined hazard scenario, earthquake intensities ranged from 0 g to 2.0 g and tsunami heights ranged from 0 m to 20 m with intervals of 0.1 g and 0.5 m, respectively, based on the combined hazard map used in Kwag et al. (2019) [3]. The combined hazard map is shown in Fig. 8. This scenario aims to simulate the simultaneous occurrence of an earthquake and a tsunami, in order to evaluate the combined effects on the safety of NPPs. The capacities of the each MACST facilities are varied within the range of 0.1 g to 3.0 g for earthquake and 0.5 m to 30 m for tsunami with intervals of 0.1 g and 0.5 m, respectively.

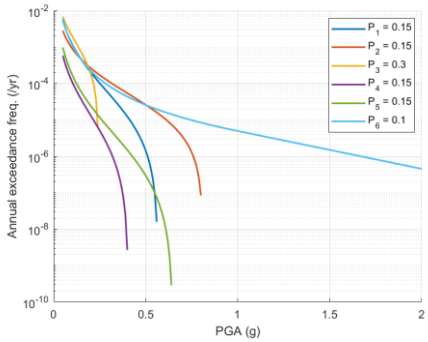

Fig. 7. Hazard curves for single seismic hazard scenario.

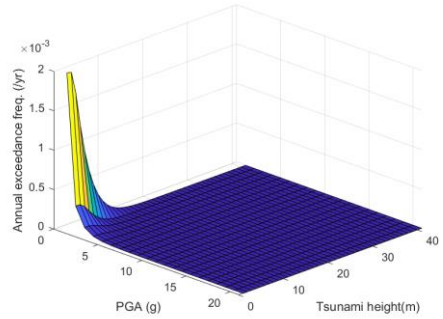

Fig. 8. Hazard map for combined earthquake-tsunami hazard scenario.

3. Results of Risk Assessment under Single and Combined Hazards

3.1 Results for Single Seismic Hazard

Fig. 9 illustrates the effect of varying the seismic capacity of the MACST facilities on the core damage (CD) risk. As the seismic capacity increases, the risk decreases significantly. The red line, representing the moving average, shows a clear trend of risk reduction as the Peak Ground Acceleration (PGA) increases up to 3.0 g, demonstrating the effectiveness of the MACST facilities in enhancing the seismic resilience of the OPR1000 system. The reduction trend begins to plateau around 1.5g, suggesting that this is the optimal seismic capacity. At this optimal capacity, the result shows a reduction in the CD risk of approximately 23%.

Fig. 10 compares the fragility curves for the OPR1000 system with and without MACST implementation. The fragility curve for the MACST-implemented system with the optimal capacity of 1.5 g shows a significant reduction in failure probability compared to the system without MACST. Specifically, the core damage probability at a seismic intensity of 1 g decreases from approximately 0.917 to 0.276, highlighting the significant risk reduction achieved through the implementation of MACST facilities.

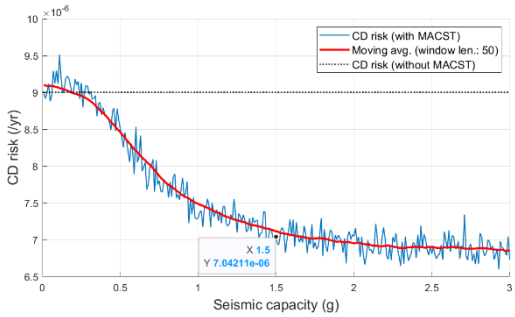

Fig. 9. Effect of seismic capacity of MACST facilities on CD risk for OPR1000.

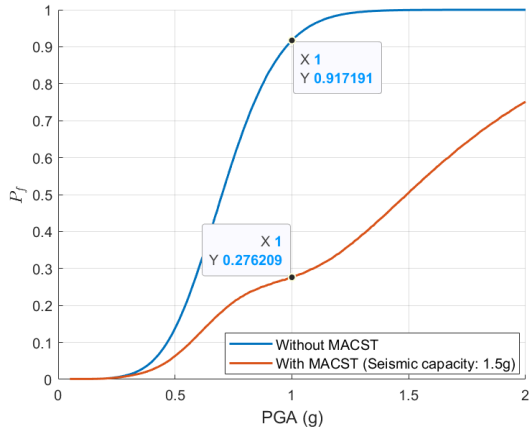

Fig. 10. Fragility curves for OPR1000 without and with MACST implementation under single hazard scenario.

Fig. 11 illustrates the effect of varying the seismic capacity of the MACST facilities on the CD risk for the APR1400. As the seismic capacity increases, the risk decreases significantly. The moving average also shows a clear trend of risk reduction as the PGA increases, and the trend begins to plateau around 1.5g, suggesting that this is the optimal seismic capacity of MACST facilities. At this optimal capacity, result shows a reduction in the CD risk of approximately 17%.

Fig. 12 shows a comparison of the fragility curves for the APR1400 system with and without the implementation of MACST. The fragility curve for the MACST-implemented system at the optimal 1.5 g capacity shows a significant reduction in failure probability compared to the system without MACST. Specifically, the core damage probability at a 1 g seismic intensity decreases from approximately 0.530 to 0.091, which indicates the significant risk reduction achieved through the implementation of MACST facilities.

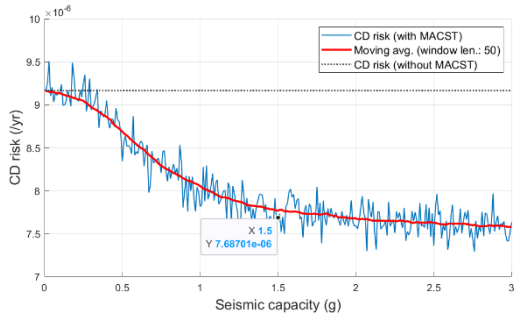

Fig. 11. Effect of seismic capacity of MACST facilities on CD risk for APR1400.

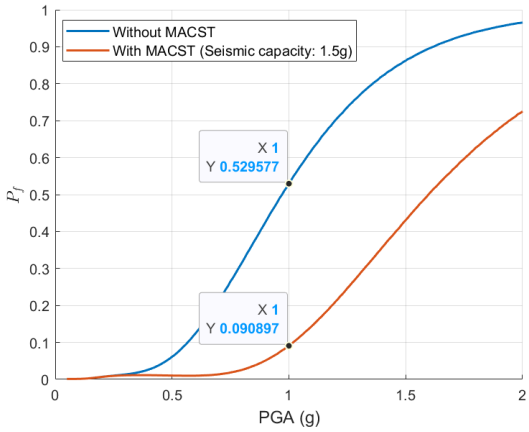

Fig. 12. Fragility curves for APR1400 without and with MACST implementation under single hazard scenario.

3.2 Results for Combined Earthquake-Tsunami Hazard

As shown in Figs. 9 through 12, the implementation of MACST facilities significantly reduces the risk to NPP systems in single seismic hazard scenario. The results show that MACST facilities significantly improve the seismic resilience of both OPR1000 and APR1400 systems. The risk of core damage is significantly reduced with optimal seismic capacity, highlighting the effectiveness of MACST facilities in mitigating the effects of seismic events and ensuring the stability and safety of NPP systems during seismic hazard event.

Fig. 13 illustrates the effect of combined earthquake and tsunami hazard on CD risk. The 3D surface plot shows how the CD risk varies with different combinations of PGA and tsunami height. As the seismic and tsunami capacities increase, the CD risk decreases significantly. Here, the risk reduction effect of the tsunami capacity compared to the seismic capacity of the MACST facilities is more significant because LEP that have the greatest impact on the CD risk is dominated by the tsunami capacity. The optimal capacities for seismic and tsunami resistance are identified as 1.5g and 10m, respectively, as these values correspond to a plateau in the risk reduction trend. At the optimal capacity, the result shows that the risk reduction is approximately 75%, demonstrating the critical role of MACST facilities in multi-hazard scenarios.

Fig. 14 compares the fragility surfaces for the OPR1000 system with and without MACST implementation under combined hazard. Fig. 14(a) shows the fragility surface for the system without MACST, and Fig. 14(b) shows the fragility surface for the MACST-implemented NPP system with the optimal capacities (1.5g seismic capacity and 10m tsunami capacity). The fragility surface for the MACST-implemented system shows a significant reduction in failure probability compared to the system without MACST. Specifically, at a seismic intensity of 1g and a tsunami height of 10m, the core damage probability decreases from approximately 0.997 to 0.529.

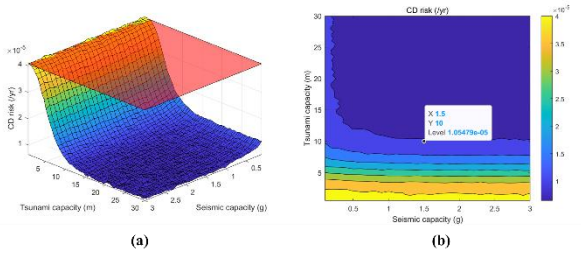

Fig. 13. Fig. 13. Effect of seismic and tsunami capacity of MACST facilities on CD risk for OPR1000 viewed as (a) 3D; and (b) 2D.

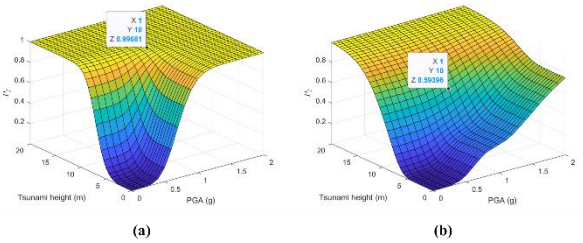

Fig. 14. Fragility surfaces for OPR1000 (a) without; and (b) with MACST implementation under combined hazard scenario.

Fig. 15 illustrates the impact of combined earthquake and tsunami hazards on the CD risk for the APR1400. The 3D surface plot shows how the CD risk varies with different combinations of PGA and tsunami height. As the seismic and tsunami capacities increase, the CD risk decreases significantly. The risk reduction effect of the tsunami capacity is also more significant compared to the seismic capacity of the MACST facilities. The optimal capacities for seismic and tsunami resistance are also identified as 1.5g and 10m, respectively, as these values correspond to a plateau in the risk reduction trend, showing that the MACST facilities are essential in managing the combined effects of these hazards.

Fig. 16 compares the fragility surfaces for the APR1400 system with and without MACST implementation under combined hazard scenarios. Fig. 16(a) shows the fragility surface for the system without

MACST, and Fig. 16(b) shows the fragility surface for the MACST-implemented system with the optimal capacities. The fragility surface for the MACST-implemented system shows a significant reduction in failure probability compared to the system without MACST. Specifically, at a seismic intensity of 1g and a tsunami height of 10m, the core damage probability decreases from approximately 0.996 to 0.530, highlighting the significant risk reduction achieved through the implementation of MACST facilities.

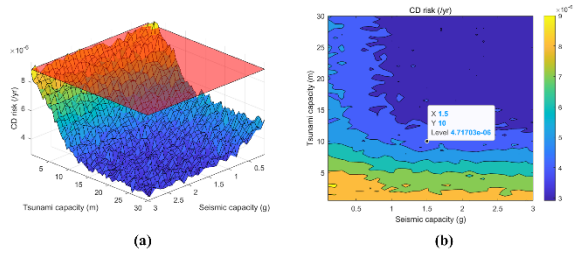

Fig. 15. Fig. 13. Effect of seismic and tsunami capacity of MACST facilities on CD risk for APR1400 viewed as (a) 3D; and (b) 2D.

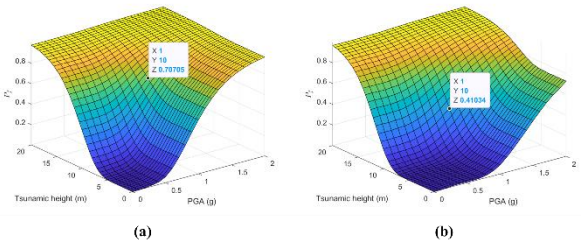

Fig. 16. Fragility surfaces for APR1400 (a) without; and (b) with MACST implementation under combined hazard scenario.

4. Conclusions

This study quantitatively demonstrated that the implementation of MACST facilities can effectively reduce the risk to NPPs under both single seismic and combined earthquake-tsunami hazards. Utilizing the I-DQFM method, this research highlighted the significant risk reduction achieved by incorporating MACST facilities into the OPR1000 and APR1400 systems. Based on the risk reduction results, optimal values for seismic and tsunami capacities of MACST facilities were also proposed to establish effective safety criteria under extreme disaster conditions.

For single hazard scenarios, the optimal seismic capacity standard of 1.5g significantly reduced the core damage probabilities for both NPP systems. Specifically, for the OPR1000 system, the implementation of MACST reduced the core damage risk by approximately 23% and the core damage fragility by approximately 72% at a 1.0g seismic intensity. Similarly, the APR1400 system experienced a reduction in risk and fragility of approximately 17% and 44%, respectively, under the same conditions.

In the context of combined earthquake and tsunami hazards, the study identified optimal capacity standards of 1.5g for seismic capacity and 10m for tsunami capacity. Under these conditions, the core damage risk was reduced by approximately 75% and the fragility was reduced by approximately 40% for the OPR1000 system at 1g seismic intensity and 10m tsunami height. Similarly, the APR1400 system experienced a reduction in risk and fragility of approximately 47% and 30%, respectively, under the same conditions. These results demonstrate the effectiveness of MACST facilities in mitigating the combined effects of earthquakes and tsunamis, and their essential role in maintaining core cooling and power during such complex disaster scenarios.

This study highlights the need for continuous improvement and adaptation of MACST facilities to address emerging threats and challenges. As climate change continues to affect the frequency and intensity of natural disasters, nuclear safety methods and strategies must evolve accordingly. Future research should focus on expanding the scope of multi-hazard risk assessments to include other potential threats such as flooding, extreme weather events, and man-made hazards. Continuous evaluation and improvement of safety measures are essential to ensure the long-term sustainability and safety of NPPs in a changing world.

Acknowledgements: This research was supported by the National Research Foundation of Korea (NRF) grant funded by the Korean government (Ministry of Science and ICT) (No. RS-2022-00154571).

REFERENCES

[1] Nuclear Energy Institute (NEI), *NEI 12-06 Rev 2 Diverse and Flexible Coping Strategies (FLEX) Implementation Guide*, December 2015.
[2] Y. Watanabe, T. Oikawa, and K. Muramatsu, Development of the DQFM Method to Consider the Effect of Correlation of Component Failures in Seismic PSA of Nuclear Power Plant, *Reliability Engineering & System Safety*, Vol.79, p.265-279, 2003.
[3] S. Kwag, J. G. Ha, M. K. Kim, and J. H. Kim, Development of Efficient External Multi-Hazard Risk Quantification Methodology for Nuclear Facilities, *Energies*, Vol.12, p.3925, 2019.
[4] J. W. Reed, M. W. McCann Jr., J. Iihara, H. Hadidi-Tamjed, Analytical techniques for performing probabilistic seismic risk assessment of Nuclear Power Plants, *Proceedings of Fourth International Conference on Structural Safety and Reliability (ICOSSAR'85)*, 1985.
[5] S. Eem, I. K. Choi, S. L. Cha, and S. Kwag, Seismic Response Correlation Coefficient for the Structures, Systems and Components of the Korean Nuclear Power Plant for Seismic Probabilistic Safety Assessment, *Annals of Nuclear Energy*, Vol.150, p.107759, 2021.
[6] B. Ellingwood, Validation Studies of Seismic PRAs, *Nuclear Engineering and Design*, Vol.123, p.189-196, 1990.